Journal of Fluorescence (2019) 29:1311–1320
https://doi.org/10.1007/s10895-019-02455-4

ORIGINAL ARTICLE

Photoinduced Reversible Modulation of Fluorescence of CdSe/ZnS Quantum Dots in Solutions with Diarylethenes

P. V. Karpach[1] · **A. A. Scherbovich**[2] · **G. T. Vasilyuk**[1] · **V. I. Stsiapura**[1] · **A. O. Ayt**[3] · **V. A. Barachevsky**[3] · **A. R. Tuktarov**[4] · **A. A. Khuzin**[4] · **S. A. Maskevich**[2]

Received: 19 September 2019 / Accepted: 31 October 2019 / Published online: 12 November 2019

Abstract

Steady-state absorption and fluorescence spectra, fluorescence decay kinetics of CdSe/ZnS quantum dots (QD) with photochromic diarylethenes (DAE) in toluene have been studied. Two kinds of QDs emitting at 525 and 600 nm were investigated and DAE were selected to ensure good overlap of their photoinduced absorption band with QDs emission spectra. It has been found that photochromic molecules form complexes with QD which results in partial fluorescence quenching. A reversible modulation of QDs emission intensity which correlates with magnitude of transient photoinduced absorption band of the diarylethenes during photochromic transformations has been demonstrated.

Keywords Quantum dots · Diarylethenes · Photochromism · Nanophotoswitches

Introduction

Photochromic compounds, reversibly changing their spectral properties under light irradiation, are attractive compounds that have great potential for development of devices for molecular electronics and photonics, and can be used as various types of photoswitches [1]. Photoinduced changes in the absorption spectra can be used in adaptive and photocontrolled light filters, to record and store information, as well as for fully optical reversible modulation of light intensity.

Reversible photoconversions of a photochromic group within bichromophoric molecular systems or complexes containing a fluorophore and the photochromic compound, can lead to fluorescence intensity modulation via 1) alteration of emission quantum yield of the fluorophore as a result of Förster resonance energy transfer (FRET) to the photochromic molecule or 2) due to reabsorption of fluorescence by the photochromic compound (inner filter effect) [2–6].

Semiconductor quantum dots (QDs) CdSe/ZnS were used as fluorophores in this work because of their photophysical properties important for practical applications [7–18]: wide spectral range of excitation, narrow emission bands, high brightness and quantum yield, great photostability, possibility to tune optical parameters (positions of absorption and fluorescence bands) by changing size of the nanoparticle.

Nowadays, QDs are widely used in diagnostic applications and biomedicine as fluorescent labels and probes [19–22] and in photovoltaics [23–26]. Possibility to tune fluorescence band wavelength and ease of obtaining thin-layer coatings using colloidal QDs is important for creating energy-efficient light-emitting devices with electric excitation QD-OLED [27, 28] and flat TV screens based on them. One of the promising areas of application for colloidal QDs is development of solar cells [29, 30].

This study is the continuation of our previous investigations [31–35] devoted to development of nanophotoswitches based on QDs and photochromic compounds from the class of diarylethenes (DAE). We studied toluene solutions of two types of CdSe/ZnS QDs in presence of DAE, which were characterized by photoinduced absorption bands having good overlap with QD fluorescence spectra – one of conditions of

---

Electronic supplementary material The online version of this article (https://doi.org/10.1007/s10895-019-02455-4) contains supplementary material, which is available to authorized users.

✉ V. I. Stsiapura
stsiapura@gmail.com

[1] Yanka Kupala State University of Grodno, Grodno, Belarus

[2] Belarusian State University, ISEI BSU, Minsk, Belarus

[3] Photochemistry Center, FSRC "Crystallography and Photonics", RAS, Moscow, Russia

[4] Institute of Petrochemistry and Catalysis, RAS, Ufa, Russia

efficient FRET. One of the photochromic compounds contained a thiol group to evaluate the effect of specific interactions on efficiency of photochromic molecules adsorption on the surface of ZnS layer of QD. Effect of photochromic transformations of DAE on fluorescence intensity and decay lifetime for CdSe/ZnS QDs of two sizes, emitting at 525 and 600 nm, was studied in toluene using steady-state and time-resolved fluorescence spectroscopy methods.

Experimental Methods

Objects of this study were CdSe/ZnS QDs as well as photochromic compounds of diarylethene class. Parameters of absorption and emission spectra for these objects were measured using spectrophotometry and fluorescence spectroscopy methods. QD samples with emission band at 525 nm (QD525) were kindly provided by Prof. Artemyev M.V. (BSU), and QDs with emission band at 600 nm (QD 600) were purchased from "Evident Tech". Molar extinction coefficients at the longwavelength absorption peak of QD525 and QD600 were $5 \cdot 10^4$ and $28 \cdot 10^4$ M^{-1} cm^{-1} respectively. Trioctylphosphineoxide (TOPO) adsorbed on QD surface after synthesis was removed by precipitation in methanol. For this, 20–30 μl of QD solution was mixed with 2 ml of methanol and vortexed until a cloudy suspension was formed. The suspension was centrifuged at 4000 rpm during 5 min, supernatant was discarded and precipitate was dissolved in toluene. Solutions of QD in toluene were mixed with DAE to obtain the needed molar ratio of QD to DAE.

Two kinds of DAE were used as photochromic compounds: DAE1 synthesized by us and DAE2 [36].

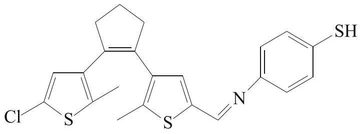

DAE1

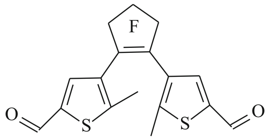

DAE2

DAE1 was synthesized by reaction of an aldehyde derivative of diarylethene DAE1′ with 4-mercaptoaniline (Scheme 1).

The aldehyde derivative DAE1′ was synthesized according to the procedure described elsewhere [37]. 4-mercaptoaniline (136 mg, 1.08 mmol) was added to a solution of diarylethene DAE1′ (350 mg, 1.08 mmol) in dry ethanol (30 ml) at room temperature. The reaction mixture was boiled for 2–3 h. The solvent was evaporated using a rotary evaporator. The product yield was about 100%.

In contrast to DAE2 compound, DAE1 contains an active thiol group, which can participate in specific interactions of DAE1 molecule with Zn and S atoms on QD surface resulting in formation of a complex.

Photochromism of DAE is based on reversible valence isomerization, i.e. in a photoinduced transition from the open form A to the cyclic form B (Scheme 2). The open colorless isomer DAE(A), after absorbing UV radiation, is converted into the cyclic colored isomer DAE(B), which, under irradiation with visible light, is transformed back to the original open isomer DAE(A). These transformations occur only under the action of light absorbed by the corresponding forms. They are considered to be thermally irreversible, since thermal relaxation of the photoinduced cyclic isomer DAE(B) to the original open form DAE(A) does not proceed at room temperature.

Absorption spectra in UV and visible ranges (200–900 nm) were recorded using SPECORD 200 spectrophotometer (Analytic Jena, Germany). We neglected possible light losses due to scattering and reflection from samples during absorption measurements. Fluorescence spectra were measured using SM2203 spectrofluorimeter (Solar, Belarus).

Time-resolved fluorescence measurements were carried out using time-correlated photon counting (TCSPC) method [38, 39] with the setup described previously [40, 41]. Briefly, picosecond PDL 800B diode laser with LDH-405 and LDH-470 laser heads (PicoQuant, Germany) generating light pulses with a typical duration of 70 ps, repetition frequency up to

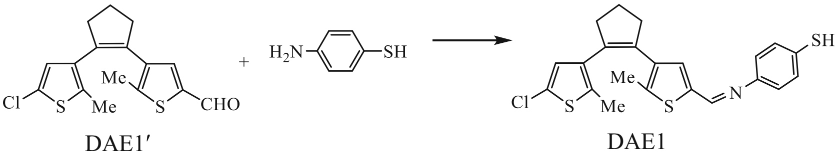

Scheme 1 Scheme of DAE1 synthesis

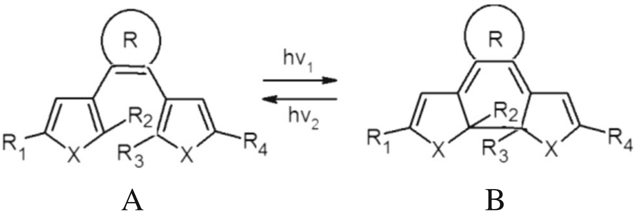

Scheme 2 Reversible photochromic isomerization in diarylethenes

40 MHz at wavelengths of 407 nm and 467 nm, respectively, was used for excitation. The detection system included PMA-182 photodetector unit as well as TCSPC board TimeHarp200 from PicoQuant (Germany). Fluorescence decay curves were recorded with a sampling step of 36 ps. Width of the instrument response function (IRF), i.e. FWHM of the exciting pulse recorded by the setup, was ~0.3 ns. Data analysis employing deconvolution of decay curves allowed to achieve time resolution of ~ 0.1 ns for TCSPC spectrometer. Iterative reconvolution method using Marquardt algorithm was used to analyze the experimental data [42–45]. Fluorescence decay function was described by a set of exponentials $F(t)=\sum_i \alpha_i exp(-t/\tau_i)$. In case of a multi-exponential decay, average lifetime <τ> was estimated according to the following expression

$$<\tau>=\frac{\sum_i \alpha_i\tau_i^2}{\sum_i \alpha_i\tau_i}, \tag{1}$$

where a_i, τ_i – preexponential factor and lifetime of the *i*- component, respectively. Parameter χ^2 was used as a goodness-of-fit criterion.

LEDs with maxima of emission bands at 365 nm (LED 365), 514 nm (LED 514) and 627 nm (LED 627) were used for irradiation of the samples. FWHM of the emission bands were 9 nm, 32 nm, 16 nm, and optical power was 0.45 W, 3 W and 3 W, respectively for LED 365, LED 514 and LED 627. Exposition time needed to convert DAE between A and B forms was determined on the base of absorption spectra measured at equilibrium conditions.

Efficiency of energy transfer (FRET) between CdSe/ZnS QDs and photochromic molecules DAE, Förster radii R_0 for the donor-acceptor pairs were estimated using set of developed programs. Based on data about fluorescence spectra of QDs, absorption spectra of DAE, an estimate of fluorescence quantum yield for QD, Förster radii were calculated in angstroms (Å) according [46] to the eq. (2).

$$R_0=0.211\left(\kappa^2n^{-4}Q_DJ(\lambda)\right)^{1/6}, \tag{2}$$

where κ^2 is the orientation factor describing mutual orientation of transition dipole moments of the donor and acceptor and assumed to be 2/3; *n* - refractive index of the medium; Q_D – fluorescence quantum yield of the donor in absence of the acceptor, *J (λ)* – an overlap integral, showing degree of overlap between emission spectra of the donor and absorption of the acceptor (3).

$$J(\lambda)=\int_0^\infty F_d(\lambda)\varepsilon_a(\lambda)\lambda^4d\lambda, \tag{3}$$

where $F_d(\lambda)$ – area normalized fluorescence spectrum of the donor; $\varepsilon_a(\lambda)$ – molar extinction coefficient of the acceptor.

Quantum yield of QD fluorescence was determined by Williams method [47] using Rhodamine 6G in ethanol as a standard. The measured fluorescence quantum yields of QD525 and QD600 in toluene in absence of acceptors were φ = 0.63 and 0.35, respectively.

Results and Discussion

The experimental data presented in Fig. 1 show good overlap for the absorption spectrum of the cyclic form B of compound DAE1 with QD525 fluorescence spectrum, and for the absorption spectrum of the cyclic form DAE2(B) with QD600 emission spectrum. Thus, there are two donor-acceptor pairs QD525-DAE1 and QD600-DAE2, which are convenient spectrally for observation of an efficient FRET. Initially, the DAE molecules are in the open form A (lacking absorption band in the range of 450–650 nm) and QDs fluorescence is not expected to be quenched by FRET. UV irradiation of the solution results in formation of the cyclic form B of DAE molecules and probability of quenching of QDs fluorescence by DAE(B) appears, depending on distance between the donor and acceptor.

Based on the spectral data (Fig. 1), values of Förster critical radii were calculated to be equal to R_0 = 4.65 nm (for QD525-DAE1(B) pair) and R_0 = 4.85 nm (for QD600-DAE2(B) pair).

In the case of FRET, intensity dependence of QD fluorescence on distance *r* between donor (QD) and acceptor (DAE) should obey the following expression:

$$I_{QD}=1-\frac{R_0^6}{r^6+R_0^6} \tag{4}$$

Fig. S1c shows distance dependence of I_{QD} for QD600-DAE2 pair having R_0 = 4.85 nm, and one can see that efficient fluorescence quenching and decrease in fluorescence quantum yield can occur only when distance between the donor QD600 and the acceptor DAE2(B) is less than 8 nm, i.e. mainly for DAE molecules near the surface of QD or adsorbed on it.

Absorption and fluorescence spectra of QDs in toluene in the presence of DAE were measured for various molar ratios of DAE: QD before and after UV irradiation. Absorption spectra of QD525 and DAE1 in toluene at molar ratio DAE 1:

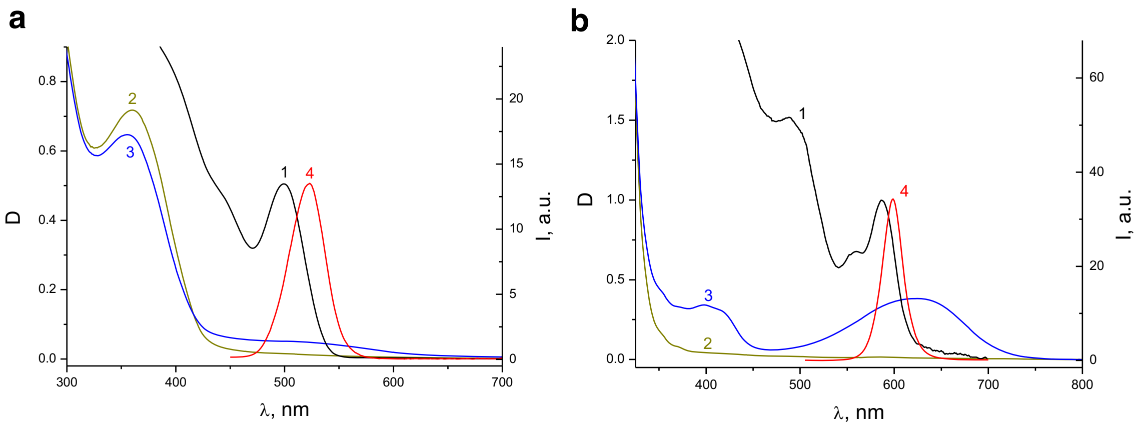

Fig. 1 Absorption spectra of QD (1), DAE in the open A (2) and cyclic B (3) forms, and QD fluorescence spectra (4) in toluene for donor - acceptor pairs DAE1-QD525 (**a**) and DAE2-QD600 (**b**)

QD = 10: 1 are shown in Fig. 2a, and similar spectra for QD600-DAE2 system (DAE 2: QD 600 ratio = 11,000: 1) - in Fig. 2b.

Photoinduced changes in absorption spectra of toluene solution containing QD525 and DAE1 (Fig. 2a) are similar to those observed for DAE1 solution in the absence of QD. However, the absorption band of the cyclic form is bathochromically shifted by 30 nm, which indicates chemical interaction of DAE1 molecules with QD surface.

Analogous photochromic transformations were also observed for mixture of DAE2 molecules with QD600 in toluene. As in the case of solution containing QD525 and DAE1 molecules, the absorption band of the cyclic isomer B of DAE2 molecule appears in the visible spectral range at 630 nm as a result of UV irradiation and disappears when the solution is exposed to visible light (Fig. 2b). However, unlike the solution of QD525 and DAE1, absorption band of the photoinduced DAE2(B) form does not change its position in the presence of QD or the spectral shift is insignificant. This may indicate absence of specific interactions between DAE2 and QD that affect chromophoric group. This, however, does not exclude the possibility of adsorption of DAE molecules on the surface of QDs.

As can be seen from Fig. 2, fluorescence intensity of QDs decreases after UV irradiation, leading to formation of DAE molecule in the cyclic colored form B. The subsequent irradiation with visible light, which restores the colorless open form A of DAE, leads to an increase in fluorescence intensity of QDs. The observed modulation of QD emission can be explained both by the inner filter effect (reabsorption of QD fluorescence by photochrome in form B) and by a change in the quantum yield of QD fluorescence due to FRET from QD to DAE(B).

We estimated plausible change of QD emission intensity due to inner filter effect for mixtures of QD-DAE shown in Fig. 2. It was found that inner filter effect can be responsible for 4% and 37% of intensity modulation for QD525-DAE1 and QD600-DAE2, correspondingly.

Figure 2 shows that modulation depth of QD emission depends on magnitude of absorption modulation for the

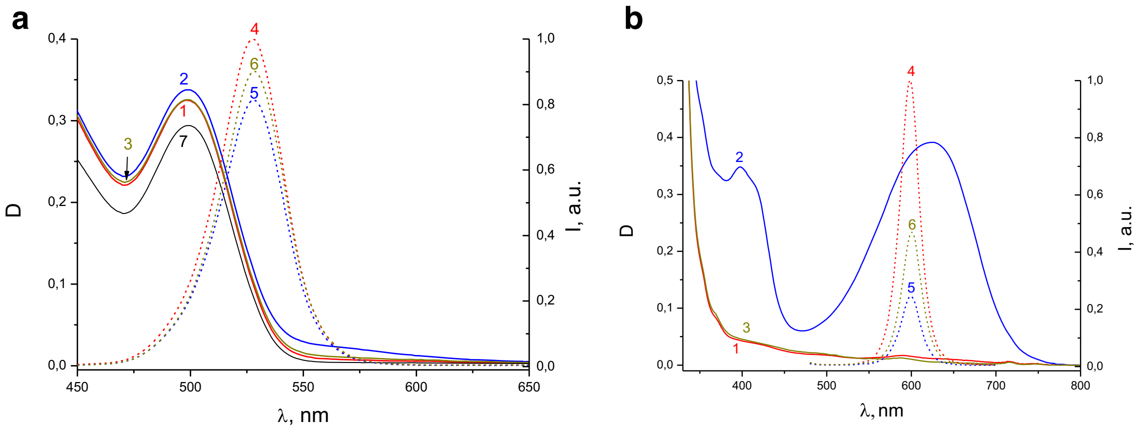

Fig. 2 Absorption (1, 2, 3) and fluorescence spectra (4, 5, 6) of QD and DAE mixture in toluene before (1, 4) and after UV radiation (365 nm) during time t_1 (2, 5), subsequent irradiation by visible light with wavelength λ_v during time t_2 (3, 6). Absorption spectrum of QD at the same concentration (without DAE) is shown by curve 7. **a** Ratio DAE1: QD525 = 10: 1 ($\lambda_v = 514$ nm, $t_1 = 200$ s, $t_2 = 45$ s), **b** Ratio DAE2: QD600 = 11,000: 1 ($\lambda_v = 627$ nm, $t_1 = 240$ s, $t_2 = 120$ s). $C_{QD525} = 6.1$ μM, $C_{QD600} = 40$ nM

photochromic compounds, therefore small modulation depth of emission intensity for QD525-DAE1 system is supposed to be related to low efficiency of photochromic transformations in DAE1 molecules. One can see that change of QD emission is not completely reversible which can be associated with restrictions to photochromic transitions in adsorbed DAE molecules or irreversible modification of QD surface after these photochromic conversions.

To get insight of the mechanism of emission modulation and features of interaction of photochromic DAE molecules with QD surface, time-resolved fluorescence of QD in the presence of initial DAE(A) and photoinduced DAE(B) forms was studied.

It should be mentioned that synthesized QD nanoparticles do not have identical structure and properties. They are characterized by size distribution of the core CdSe and the shell ZnS, as well as by degree of homogeneity of QD surface (i.e. presence of defects on the surface like dangling bonds, etc.). The latter factor has strong effect both on chemical and fluorescent properties of QD. Surface defects may lead to formation of localized electronic states or highly reactive sites, which are prone to chemical and redox processes [48]. They may play role of electron traps forming nonradiative decay channels for photoexcited QD. From the other side, surface defects are highly reactive, they can act as binding sites for dye molecules, and adsorption of molecules having electron-accepting properties (like porphyrin) on QD surface can be considered as formation of a new type of surface trap that may affect fluorescent properties [49, 50]. All the above-mentioned as well as relaxation processes related to electron-phonon interactions during thermalization of the excited state of QD results in a complicated fluorescence decay law [51–53], and even for QD solutions in absence of DAE at least three exponential components are usually needed to describe the emission decay. In this case it is difficult to assign physical meaning to decay parameters α_i, τ_i in multiexponential model and they are used merely as fitting parameters to characterize fluorescence decay and average lifetime $<\tau>$.

Figure 3 shows that the experimentally measured kinetics of QD emission decay has essentially multiexponential character and, for example, at least 3 exponential components with lifetimes of $\tau_1 \sim 1$, $\tau_2 \sim 6$ and $\tau_3 \sim 20$ ns are needed to describe fluorescence decay curves for QD525. Effect of DAE concentration for two isomeric forms A and B on QD fluorescence decay (and related to it quantum yield) was assessed by change of the average decay lifetime $<\tau>$. The results of experimental studies are presented in Fig. 4 and Tables 1, 2, and 3.

Figure 4 shows dependence of average emission decay lifetime for QD in toluene on concentration of DAE molecules in the form of isomer A, which could be potential acceptors of photoexcitation energy only after UV irradiation. One can see that addition of DAE(A) in low concentrations leads to a slight increase of the average lifetime (≤10%). Then a significant reduction of $<\tau>$ is observed upon concentration growth of the colorless DAE(A) isomer. Obviously, this behavior cannot be attributed to FRET-effect. We suggest that decrease of fluorescence lifetime of QD at high concentrations of DAE is not caused by dynamic quenching of QD emission, when a collisional complex QD-DAE can be formed during the excited state lifetime of QD and resulting in its deactivation. This is supported by the following arguments: 1) fluorescence decay kinetics for a mixture of QD and DAE depended on incubation time after mixing, 2) increase of $<\tau>$ in the range of low concentration for

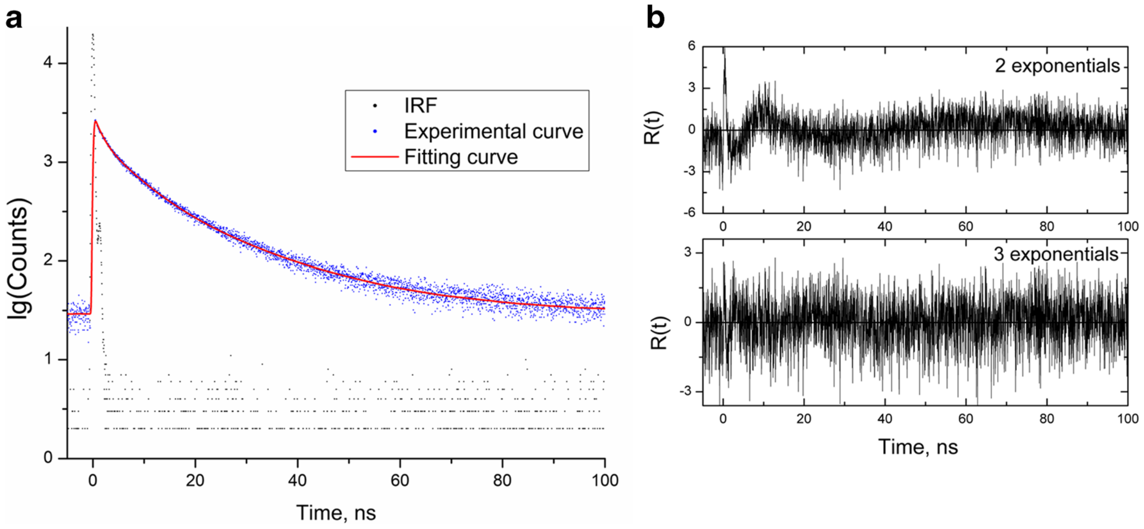

Fig. 3 Fluorescence decay curve for QD525 in toluene. **a** – IRF and decay curve are shown with dots, fitting curve – with line. **b** Plot of weighted residuals R(t) for 2 and 3 exponential fitting

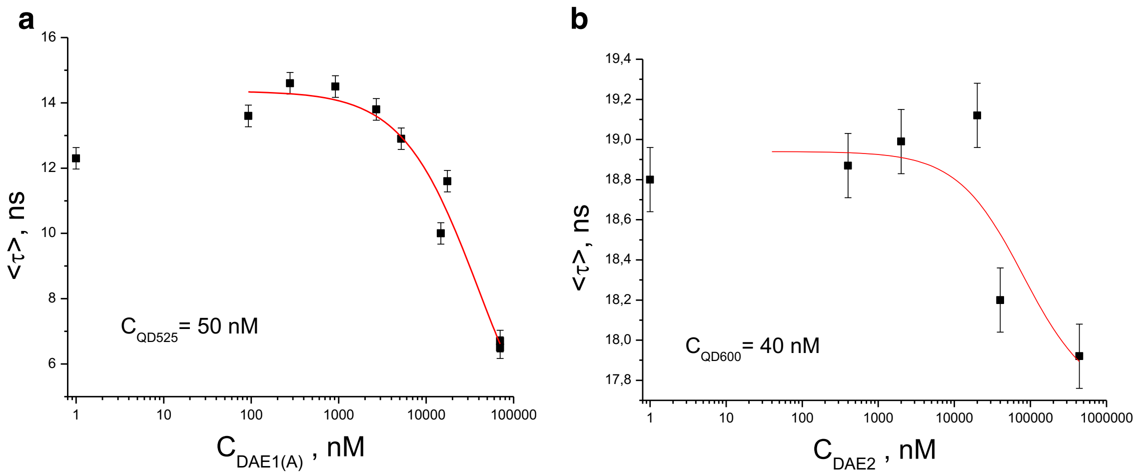

Fig. 4 Dependence of average decay lifetime for QD525 (**a**) and QD600 (**b**) fluorescence in toluene on concentration of the colorless isomer A of DAE1 (a) and DAE2 (b). $C_{QD525} = 50$ nM, $C_{QD600} = 40$ nM. $\lambda_{ex} =$ 467 nm. $\lambda_{fl} = 525$ nm (a) or 600 nm (b). Fitting using Hill model is shown with line

DAE, 3) Stern–Volmer equation for the range of high DAE concentrations gives implausibly high values for bimolecular rate constant of quenching.

Obviously, DAE1 molecule (even in the colorless form A) plays a role of a significantly more efficient quencher for QD525 fluorescence than DAE2 for QD600. Addition of high concentration of DAE1 molecules having thiol- groups in their structure resulted in significant reduction of the decay lifetime of QD emission which may indicate chemical interaction between photochromic molecules and QD surface or be related to high electron-accepting properties of DAE1. Absence of these functional groups in DAE2 compound may be related to a lower efficiency of its interaction with QDs and less significant reduction of decay lifetime for QD emission in the presence of DAE2. The idea about essentially low energy of interaction with QD surface and mainly physical adsorption of DAE2 molecules is supported by experimental data about interaction of these molecules with silver nanoparticles [54]. Sensitivity of QD fluorescence kinetics to presence of DAE molecules can also be due to different thickness and uniformity of ZnS shell for QD525 and QD600.

We suppose that specific interactions between QD525 and DAE1(A) molecules (or between QD600 and DAE2(A) molecules) giving rise to formation of QD-DAE complexes or associates are among the main reasons of QD fluorescence quenching. It is suggested that formation of a complex (or associate) results in appearance of an additional non-radiative decay channel that will lead to decrease in <τ> of QD emission, rather than complete quenching of the fluorescence. This allows us to estimate maximal value of equilibrium dissociation constant K_d (for 1:1 complex of QD: DAE) using Hill model [55] for protein-ligand interactions (5), if complex formation leads to a decrease in average lifetime of QD fluorescence from τ_0 to τ_{min},

$$\langle\tau\rangle = \tau_0 - (\tau_0 - \tau_{\min})\frac{C_{DAE}}{K_d + C_{DAE}}, \quad (5)$$

Table 1 Fluorescence decay parameters for QD525 in presence of different DAE(A) concentrations in toluene obtained by global analysis. $\lambda_{ex} =$ 467 nm, $\lambda_{fl} = 525$ nm, $S_i \sim \alpha_i \tau_i$ – contribution of i-th component in emission. $C_{QD525} = 50$ nM

C_{DAE}, nM	α_1	τ_1, ns	S_1, %	α_2	τ_2, ns	S_2, %	α_3	τ_3, ns	S_3, %	<τ>, ns	χ^2
0	0.380	1.2	7.1	0.434	5.8	39.5	0.186	18.3	53.4	12.1	1.03
93	0.283		4.3	0.448		33.1	0.269		62.6	13.4	0.99
280	0.243		3.4	0.446		30.2	0.311		66.4	13.9	1.03
920	0.274		4.0	0.435		30.9	0.291		65.1	13.7	1.06
2690	0.290		4.5	0.442		32.9	0.267		62.6	13.4	1.05
5190	0.331		5.6	0.447		36.8	0.222		57.5	12.7	1.08
14,700	0.486		11.9	0.407		48.3	0.106		39.8	10.2	1.12
17,500	0.408		8.2	0.430		41.9	0.162		49.8	11.6	1.10
70,000	0.735		31.4	0.234		48.4	0.031		20.2	6.9	1.29

Table 2 Average decay lifetimes <τ> of QD525 emission in toluene in the presence of DAE1 molecules at different molar ratios DAE1:QD525 before, after UV irradiation and subsequent exposure to visible light. $C_{QD525} = 50$ nM, $\lambda_{ex} = 467$ nm, $\lambda_{fl} = 520$ nm

Sample solution	<τ> in ns at DAE1:QD525 ratios		
	10:1	300:1	1000:1
QD525 in absence of DAE1	12.3		
Mixture of QD525 and DAE1(A) before irradiation	13.5	11.5	9.3
Mixture of QD525 and DAE1 after UV irradiation (λ = 365 nm)	11.6	6.9	4.1
Mixture of QD525 and DAE1 after subsequent irradiation with visible light (λ = 514 nm)	12.0	7.0	4.3

where C_{DAE}- concentration of the unbound ligand (DAE) in solution;

$$K_d = \frac{C_{QD} \cdot C_{DAE}}{C_{QD-DAE}}$$ –the equilibrium dissociation constant,

where C_{QD} - concentration of free QD in solution; $C_{QD\text{-}DAE}$ - concentration of QD-DAE complexes/associates in solution.

Experimental data of <τ> for QD525-DAE1(A) donor-acceptor pair within DAE1 concentration range from 100 nM to 100 μM were fitted by Hill model (Fig. 4a) and maximal value for $K_d \sim 40 \pm 20$ μM (for the 1: 1 complex) was estimated. Similar value of $K_d \sim 40$ μM was determined for QD600-DAE2(A) pair. On the base of exciton band position one can estimate that diameters of CdSe cores [56] for QD525 and QD600 are equal to ~2.5 and 4.5 nm respectively. Assuming that ZnS layer has a thickness of ~ 0.5 nm the surface area for QD600 will be ~3 times larger than the one for QD525. Therefore, one can conclude that K_d value for QD525-DAE1 complex, having the same magnitude as the one for QD600-DAE2 complex, is related to chemical nature of DAE1 molecules. Higher affinity of DAE1 to QD surface is attributed to presence of chemically active thiol groups in DAE1 molecule.

These data support our suggestion about formation of complexes/associate in toluene solutions of QD and DAE. Moreover, complex formation between photochromic molecules having substituents of different nature and QD surface can explain slight growth of the average decay lifetime at low concentrations of DAE1(A).

More detailed analysis of DAE(A) concentration on fluorescence decay of QD was performed using global analysis method [40, 44, 57], when a set of decay curves was fitted simultaneously using common lifetime parameters τ_i. This approach allows to determine how contributions (or weights) of short- and long-lived emission centers into fluorescence change upon growth of DAE amount in solution. One can see from Table 1 that addition of DAE1(A) up to ~280 nM concentration in the toluene solution of QD525 results in ~2 times decrease of emission contribution (proportional to $\alpha_i\tau_i$) for the short-lived component. We propose that in these conditions photochromic molecules will be preferentially bound to QD with more defects on their surface since these defects on ZnS layer play role of potential binding sites for DAE molecules. From the other hand, QD having more defects are usually characterized by shorter fluorescence decay lifetimes because surface defects are related to formation of electron trap states increasing rate of non-radiative deactivation for the photoexcited QD. Therefore, at low concentrations of DAE a preferential binding to QD with short-lived emission is expected to take place. This binding can be followed by QD fluorescence quenching (full or partial) that leads, in our opinion, to increase of the average fluorescence decay lifetime for QD ensemble. We do not exclude an alternative possibility – activation of QD fluorescence at these conditions due to QD surface modification upon DAE binding and destabilization of electron traps.

Further addition of DAE to QD solution is accompanied by gradual decrease of <τ> value and corresponding changes in

Table 3 Average decay lifetimes <τ> of QD600 emission in toluene in the presence of DAE2 molecules at different molar ratios DAE2:QD600 before, after UV irradiation, and subsequent exposure to visible light. $C_{QD600} = 40$ nM, $\lambda_{ex} = 467$ nm, $\lambda_{fl} = 600$ nm

Sample solution	<τ> in ns at DAE2:QD600 ratios		
	10:1	1000:1	11,000:1
QD600 in absence of DAE2	18.8		
Mixture of QD600 and DAE2(A) before irradiation	18.9	18.2	17.9
Mixture of QD600 and DAE2 after UV irradiation (λ = 365 nm)	18.0	17.3	16.2
Mixture of QD600 and DAE2 after subsequent irradiation with visible light (λ = 627 nm)	17.8	17.2	16.0

weights of short- and long-lived components of the emission due to quenching.

Effects of reversible DAE photoisomerization, manifested in absorption spectra alteration, on QD fluorescence kinetics were studied. Solutions of QD and DAE were irradiated with light of UV and visible LEDs with the same exposition times as indicated in the caption of Fig. 2. The obtained results are shown in Tables 2 and 3. It is important to mention that irradiation of QD solutions in the same conditions but in absence of DAE did not affect intensity and decay kinetics of QD emission. Irradiation of solutions with UV light, which induces the transition into the closed colored form B of DAE molecules, leads to a slight decrease of the average decay lifetime for both systems studied (Tables 2 and 3), which can be interpreted as appearance of an additional channel for the excited state decay. Answer on the question if this decay channel is related to FRET from QD to the colored DAE(B) form will depend on restore of <τ > value (full or partial) upon conversion of DAE molecules back to the initial form A.

One can see (Table 3) that visible light irradiation, which induces the transition of DAE molecules back to the open form A, does not lead to any significant changes in the average fluorescence decay lifetime for QD600-DAE2 system. In the case of QD525-DAE1 system, a slight photoinduced modulation of emission decay lifetime is observed (Table 2) after sequential irradiation with UV and visible light, which indicates that energy transfer between QD and DAE1 occurs by FRET mechanism. Dissimilarity in behavior of the two studied QD-DAE systems can be explained taking into account different sizes of QD525 and QD600.

It is noteworthy that the estimated Ferster radii for the both donor-acceptor pairs do not differ much, having values of 4.6 and 4.8 nm for QD525-DAE1 and QD600-DAE2 respectively. However, QD sizes are significantly different and the corresponding radii of QD with ZnS layer are equal to ~2 and 3 nm for QD525 and QD600. Taking into account that FRET efficiency depends on distance as $\sim 1/r^6$, it is expected that contribution of FRET process in the excited state deactivation for QD600-DAE2 system will be essentially lower than in the case of QD525-DAE1 due to the increased distance between QD center and the adsorbed DAE molecule (this value is used as a distance between the point dipoles in FRET model).

Both systems QD-DAE showed significant lowering of the average decay lifetime after first irradiation with UV light, inducing DAE transition to the colored B form, and < τ > value did not restore to the initial value after subsequent irradiation of the solution with visible light. Nature of this quenching process is not known at current stage of research and needs further investigations. We propose that the irreversible lowering of <τ > (and related to it quantum yield) for QD fluorescence could be due to formation of a stable irreversible complex QD-DAE(B) for part of the adsorbed photochromic molecules after cyclization that may play role of an effective electron trap.

The results of this study show that the reversible phototransformations of the photochromic components of QD-DAE systems under UV and visible light have little or negligible effect on modulation of decay lifetime of QDs fluorescence. Chemical nature of the adsorbed photochromic molecules and, possibly, their amount on QD surface, are the main factors affecting fluorescence decay of QDs.

Thus, according to emission decay measurements, a slight contribution of FRET in QD emission modulation was found for QD525-DAE1 system only and we suggest that the observed modulation of fluorescence intensity (Fig. 2) upon photochromic conversions of DAE molecules are mainly related to reabsorption of fluorescence due to inner filter effect.

Conclusions

Photoinduced modulation of QD fluorescence intensity was demonstrated for toluene solutions of photochromic DAE molecules with QDs of two sizes, having fluorescence bands at 525 nm and 600 nm. Change of QD emission intensity was synchronous with the changes in the photoinduced absorption of DAE molecules during their photochromic transformations. The observed modulation of fluorescence intensity is mainly associated with fluorescence reabsorption due to the inner filter effect and partially with Forster resonant energy transfer from QD to the photoinduced cyclic form B of DAE molecules. Ferster radii for donor-acceptor pairs QD525-DAE1 and QD600-DAE2 were calculated to be 4.65 nm and 4.85 nm correspondingly. According to our estimations changes in fluorescence intensity related to the reabsorption effect are equal to 4% and 37% for QD525-DAE1 and QD600-DAE2 systems respectively.

It was found that fluorescence decay lifetime of QD was sensitive to chemical properties and concentration of DAE in solution. Decrease of fluorescence decay lifetime in presence of DAE was interpreted as evidence of specific interactions of photochromic molecules with QD surface. Using emission decay kinetics data the effective dissociation constants were evaluated to be ~40 μM for both types of QD-DAE complexes. Taking into account different surface areas for QD525 and QD600 (~3 times), the higher affinity of DAE1 to QD surface is supposed to be related to presence of chemically active thiol groups in DAE1 molecule.

Acknowledgements This work was supported by Belarusian Republican Foundation for Fundamental Research (Project No. F18R-074) and Russian Foundation for Basic Research (Project No. 18-33-00010 Bel_a). The authors are grateful to Prof. M. Artemyev (Dr. of Sciences (Chemistry), Head of Laboratory of Nanochemistry, Institute of Physical and Chemical problems of BSU) for the sample of quantum dots and valuable discussions.

References

1. Feringa BL (ed) (2001) Molecular switches. Wiley Weinheim.
2. Zhang J, Zou Q, Tian H (2013) Photochromic materials: more than meets the eye. Adv Mater 25(3):378–399
3. Klajn R, Stoddart JF, Grzybowski BA (2010) Nanoparticles functionalised with reversible molecular and supramolecular switches. Chem Soc Rev 39(6):2203–2237
4. Hasegawa Y, Nakagawa T, Kawai T (2010) Recent progress of luminescent metal complexes with photochromic units. Coord Chem Rev 254(21–22):2643–2651
5. Cusido J, Deniz E, Raymo FM (2009) Fluorescent switches based on photochromic compounds. Eur J Org Chem 2009(13):2031–2045
6. Raymo FM, Tomasulo M (2005) Fluorescence modulation with photochromic switches. J Phys Chem A 109(33):7343–7352
7. Díaz SA, Menendez GO, Etchehon MH, Giordano L, Jovin TM, Jares-Erijman EA (2011) Photoswitchable water-soluble quantum dots: pcFRET based on amphiphilic photochromic polymer coating. ACS nano 5(4):2795–2805
8. Yildiz I, Deniz E, Raymo FM (2009) Fluorescence modulation with photochromic switches in nanostructured constructs. Chem Soc Rev 38(7):1859–1867
9. Yildiz I, Tomasulo M, Raymo FM (2008) Electron and energy transfer mechanisms to switch the luminescence of semiconductor quantum dots. J Mater Chem 18(46):5577–5584
10. Tomasulo M, Yildiz I, Raymo FM (2007) Nanoparticle-induced transition from positive to negative photochromism. Inorg Chim Acta 360(3):938–944
11. Binder WH, Sachsenhofer R, Straif CJ, Zirbs R (2007) Surface-modified nanoparticles via thermal and Cu (I)-mediated “click” chemistry: generation of luminescent CdSe nanoparticles with polar ligands guiding supramolecular recognition. J Mater Chem 17(20):2125–2132
12. Tomasulo M, Yildiz I, Kaanumalle SL, Raymo FM (2006) pH-sensitive ligand for luminescent quantum dots. Langmuir 22(24):10284–10,290
13. Tomasulo M, Yildiz I, Raymo FM (2006) pH-sensitive quantum dots. J Phys Chem B 110(9):3853–3855
14. Tomasulo M, Yildiz I, Raymo FM (2006) Luminescence modulation with semiconductor quantum dots and photochromic ligands. Aust J Chem 59(3):175–178
15. Jares-Erijman E, Giordano L, Spagnuolo C, Lidke K, Jovin TM (2005) Imaging quantum dots switched on and off by photochromic fluorescence resonance energy transfer (pcFRET). Mol Cryst Liq Cryst 430(1):257–265
16. Zhu L, Zhu M-Q, Hurst JK, Li AD (2005) Light-controlled molecular switches modulate nanocrystal fluorescence. JACS 127(25):8968–8970
17. Medintz IL, Trammell SA, Mattoussi H, Mauro JM (2004) Reversible modulation of quantum dot photoluminescence using a protein-bound photochromic fluorescence resonance energy transfer acceptor. JACS 126(1):30–31
18. Giordano L, Jovin TM, Irie M, Jares-Erijman EA (2002) Diheteroarylethenes as thermally stable photoswitchable acceptors in photochromic fluorescence resonance energy transfer (pcFRET). JACS 124(25):7481–7489
19. Alivisatos P (2004) The use of nanocrystals in biological detection. Nat Biotechnol 22(1):47–52
20. Medintz IL, Uyeda HT, Goldman ER, Mattoussi H (2005) Quantum dot bioconjugates for imaging, labelling and sensing. Nat. Mater. 4(6):435
21. Kairdolf BA, Smith AM, Stokes TH, Wang MD, Young AN, Nie S (2013) Semiconductor quantum dots for bioimaging and biodiagnostic applications. Annu. Rev. Anal. Chem. 6(1):143
22. Alivisatos AP, Gu W, Larabell C (2005) Quantum dots as cellular probes. Annu Rev Biomed Eng 7:55–76
23. O'regan B, Grätzel M (1991) A low-cost, high-efficiency solar cell based on dye-sensitized colloidal TiO2 films. Nature 353(6346):737
24. McDonald SA, Konstantatos G, Zhang S, Cyr PW, Klem EJ, Levina L, Sargent EH (2005) Solution-processed PbS quantum dot infrared photodetectors and photovoltaics. Nat. Mater. 4(2):138
25. Tang J, Kemp KW, Hoogland S, Jeong KS, Liu H, Levina L, Furukawa M, Wang X, Debnath R, Cha D (2011) Colloidal-quantum-dot photovoltaics using atomic-ligand passivation. Nat. Mater. 10(10):765
26. Nozik AJ, Beard MC, Luther JM, Law M, Ellingson RJ, Johnson JC (2010) Semiconductor quantum dots and quantum dot arrays and applications of multiple exciton generation to third-generation photovoltaic solar cells. Chem Rev 110(11):6873–6890
27. Dayneko S, Lypenko D, Linkov P, Sannikova N, Samokhvalov P, Nikitenko V, Chistyakov A (2016) Application of CdSe/ZnS/CdS/ZnS core–multishell quantum dots to modern OLED technology. Mater. Today: Proc. 3(2):211–215
28. Vitukhnovskii A, Vaschenko A, Bychkovskii D, Dirin D, Tananaev P, Vakshtein M, Korzhonov D (2013) Photo-and electroluminescence from semiconductor colloidal quantum dots in organic matrices: QD-OLED. Semiconductors 47(12):1567–1569
29. Huynh WU, Dittmer JJ, Alivisatos AP (2002) Hybrid nanorod-polymer solar cells. Science 295(5564):2425–2427
30. Kamat PV (2008) Quantum dot solar cells. Semiconductor nanocrystals as light harvesters. J Phys Chem C 112(48):18737–18,753
31. Barachevsky V, Kobeleva O, Ayt A, Gorelik A, Valova T, Krayushkin M, Yarovenko V, Levchenko K, Kiyko V, Vasilyuk G (2013) Optical polymer materials with photocontrolled fluorescence. Opt Mater 35(10):1805–1809
32. Barachevsky V (2015) Nanophotochromism. OPP 3(1):8–41. https://doi.org/10.1515/oph-2015-0003 ISSN:2299-3177
33. Barachevsky V (2018) Photochromic Nanoparticles and Their Properties. Crystallography Reports 63(2):271–275
34. Barachevsky V (2018) Advances in photonics of organic photochromism. J Photochem Photobiol A: Chem 354:61–69
35. Barachevsky V, Kobeleva O, Venidiktova O, Ayt A, Vasilyuk G, Maskevich S, Krayushkin M (2019) Photoinduced modulation of emission of quantum dots CdSe/ZnS by photochromic transformation of diarylethenes. Crystallogr. Rep. 64(5):823–827
36. Barachevsky V, Krayushkin M, Kiyko V (2017) Light-Sensitive Organic Recording Media for Three-Dimensional Optical Memory. Photon-Working Switches. Springer, In, pp 181–207
37. Tuktarov AR, Khuzin AA, Akhmetov AR, Barachevsky VA, Venidiktova OV, Dzhemilev UM (2015) Synthesis and photochromic properties of fullerene C60 adducts with dithienylethenes. Tetrahedron Lett 56(52):7154–7157
38. Wahl M (2014) Modern TCSPC electronics: principles and acquisition modes. In: Advanced Photon Counting. Springer, pp. 1–21.
39. O'Connor DV, Phillips D (1984) Time-correlated Single Photon Counting. Academic Press, New York
40. Maskevich A, Stepuro V, Kurguzenkov S, Lavysh A (2013) Hardware and software complex for fluorescence decay studies.

Vesnik of Yanka Kupala State University of Grodno (in Russian) 159(3):107-119 ISSN:2076-4847
41. Stsiapura VI, Maskevich AA, Kuzmitsky VA, Uversky VN, Kuznetsova IM, Turoverov KK (2008) Thioflavin T as a molecular rotor: fluorescent properties of thioflavin T in solvents with different viscosity. J Phys Chem B 112(49):15893–15902. https://doi.org/10.1021/jp805822c
42. Bevington PR, Robinson DK (1969) Data reduction and error analysis for the physical sciences, vol 336 McGraw-Hill New York
43. Yuan Y-X (2011) Recent advances in numerical methods for nonlinear equations and nonlinear least squares. NACO 1(1):15–34 ISSN:2155-3289
44. Stepuro V (2001) Studies of fluorescence decay for multicomponent systems using global analysis. Vesnik of Yanka Kupala State University of Grodno (in Russian) 5 (1):52-61 ISSN:2076-4847
45. Johnson ML, Frasier SG (1985) Nonlinear least-squares analysis. In: Methods in Enzymology, vol 117. Elsevier, pp. 301–342.
46. Lakowicz JR (2013) Principles of fluorescence spectroscopy. Springer Science & Business Media,
47. Williams ATR, Winfield SA, Miller JN (1983) Relative fluorescence quantum yields using a computer-controlled luminescence spectrometer. Analyst 108(1290):1067–1071
48. Giansante C, Infante I (2017) Surface traps in colloidal quantum dots: a combined experimental and theoretical perspective. J Phys Chem Lett 8(20):5209–5215
49. Zenkevich E, Stupak A, Göhler C, Krasselt C, von Borczyskowski C (2015) Tuning electronic states of a CdSe/ZnS quantum dot by only one functional dye molecule. ACS nano 9(3):2886–2903
50. Zenkevich EI, Blaudeck T, Milekhin A, Von Borczyskowski C (2012) Size-Dependent non-FRET photoluminescence quenching in nanocomposites based on semiconductor quantum dots CdSe/ZnS and functionalized porphyrin ligands. Int. J. Spectrosc. 2012: 971791. https://doi.org/10.1155/2012/971791
51. Schlegel G, Bohnenberger J, Potapova I, Mews A (2002) Fluorescence decay time of single semiconductor nanocrystals. Phys Rev. Lett 88 (13):137401.
52. Wang H, de Mello DC, Meijerink A, Glasbeek M (2006) Ultrafast exciton dynamics in CdSe quantum dots studied from bleaching recovery and fluorescence transients. J Phys Chem B 110(2):733–737
53. Knowles KE, McArthur EA, Weiss EA (2011) A multi-timescale map of radiative and nonradiative decay pathways for excitons in CdSe quantum dots. Acs Nano 5(3):2026–2035
54. Kobeleva O, Valova T, Barachevskii V, Krayushkin M, Lichitskii B, Dudinov A, Kuznetsova OY, Adamov G, Grebennikov E (2010) Spectral-kinetic evidence of interaction of photochromic diarylethenes with silver nanoparticles. Opt Spectrosc 109(1): 101–105
55. Cantor CR, Schimmel PR (1980) Biophysical chemistry: Part III: the behavior of biological macromolecules. Macmillan,
56. Yu WW, Qu L, Guo W, Peng X (2003) Experimental determination of the extinction coefficient of CdTe, CdSe, and CdS nanocrystals. Chem Mater 15(14):2854–2860
57. Knutson JR, Beechem JM, Brand L (1983) Simultaneous analysis of multiple fluorescence decay curves: a global approach. Chem Phys Lett 102(6):501–507